Tuning the Photophysical and Electrochemical Properties of Aza-boron-dipyridylmethenes for Fluorescent Blue OLEDs

Abegail C. Tadle,[1] Karim A. El Roz,[1] Chan Ho Soh,[2] Daniel Sylvinson Muthiah Ravinson,[1] Peter I. Djurovich,[1] Stephen R. Forrest,[2,3,4] Mark E. Thompson[1,5,*]

[1] Department of Chemistry, University of Southern California, Los Angeles, California, 90089, USA

[2] Department of Physics, University of Michigan, Ann Arbor, Michigan 48109, USA

[3] Department of Electrical and Computer Engineering, University of Michigan, Ann Arbor, Michigan 48109, USA

[4] Department of Materials Science and Engineering, University of Michigan, Ann Arbor, Michigan 48109, USA

[5] Mork Family Department of Chemical Engineering and Materials Science, University of Southern California, Los Angeles, California, 90089, USA

A. C. Tadle, Dr. K. A. El Roz, D. S. M. Ravinson, Dr. P. I. Djurovich, Dr. M. E. Thompson.

Department of Chemistry, University of Southern California, Los Angeles, California, 90089, USA

E-mail: met@usc.edu

C. H. Soh, Dr. S. R. Forrest

Department of Physics, University of Michigan, Ann Arbor, Michigan 48109, USA

Keywords: organic light-emitting diodes, photoluminescence, organic electronics, optically active materials, thin film doping

Abstract

* To whom correspondence should be addressed. Email: met@usc.edu

A series of substituted boron aza-dipyridylmethene (**aD**) compounds are demonstrated as fluorescent dopant emitters in blue organic light emitting diodes (OLEDs). Replacing the *meso*-carbon of a dipyridylmethene dye with nitrogen to form the **aD** chromophore leads to a destabilization of the highest occupied molecular orbital in **aD**, as evidenced both from their experimentally determined photophysical and electrochemical properties. These properties are consistent with theoretical calculations of the molecular energetics. These **aD** derivatives emit violet to blue light, peaking between 400 and 460 nm with photoluminescent quantum yields over 85%. The **aD** compounds have small energy differences (< 400 meV) between their singlet and triplet excited states. OLEDs fabricated with an aza-boron-dipyridylmethene emitting fluorophore give an external quantum efficiency of 4.5% on glass substrates, close to the theoretical maximum for fluorescent OLEDs.

1. Introduction

Organic light emitting diodes (OLEDs) have been commercialized for use in the displays of mobile phones, tablets, televisions, and wearable technologies, as well as in solid-state lighting panels. The electroluminescent process involves hole/electron recombination that leads to a mixture of singlet and triplet excitons.[1] In the late 1990's, phosphorescent emitters were incorporated into OLEDs, making it possible to harvest both types of excitons and achieve 100 % internal efficiency for conversion of electrical charges into photons. OLEDs with green and red phosphorescent emitters have been shown to achieve both high quantum efficiencies and long device lifetimes, and have thus become standard emissive dopants in commercial OLED displays.[2] While the internal quantum efficiencies of OLEDs utilizing blue phosphorescent dopants have also reached the theoretical limit of 100%, the operational lifetimes of these devices have thus far been short and can be improved for practical application in displays.[3] The stability of blue phosphorescent OLEDs is limited by degradation of the host and/or dopant materials via bimolecular decay processes, *i.e.* exciton-exciton or exciton-polaron annihilation.[3j, 4] These second order processes are exacerbated by the long excited state decay lifetimes of phosphorescent emitters, typically a few microseconds. Fluorescent blue emitters are less efficient in OLEDs, but their markedly shorter excited state lifetimes (nanoseconds) dramatically reduce the rate of bimolecular decay, thereby increasing the device operational lifetime. Thus, fluorescence-based blue dopants are conventionally used for OLEDs in commercial displays.

Blue fluorescent materials also have utility in white OLEDs (WOLEDs) for solid state lighting.[5] Our interest in blue fluorophores stems from a device architecture that splits the singlet and triplet excitons spatially within the WOLED, allowing for the singlet excitons to be harvested on a blue

fluorescent dopant and the triplets on red and green phosphorescent dopants.[5-6] This hybrid fluorescent/phosphorescent WOLED has the potential to give high color quality with an internal quantum efficiency of 100%, without the need for blue phosphors. However, aside from highly efficient blue luminescence, the energy of the triplet state of the fluorescent dopant in this architecture needs to be high enough to enable endothermic energy transfer to the green-to-red phosphorescent dopant. This requirement places a restriction on the most common structural motifs used to create fluorescent blue lumiphores (stilbenes, anthracenes, etc.), as energies for the triplet state in these materials is typically too low (E_T < 2 eV) for effective energy transfer to the phosphor. Moreover, the hybrid WOLED puts a further restriction on the fluorophore in that it needs to have a blue emissive singlet and a high triplet energy, thus requiring a small energy difference between the singlet and triplet excited states (ΔE_{ST}), preferably with ΔE_{ST} < 400 meV.

Here, we focus on demonstrating a **DIPYR** (boron dipyridylmethene, **Figure 1**) family of dyes[7] to achieve highly efficient blue fluorescence in OLEDs. **DIPYR** dyes are related to the more widely studied BODIPY (4,4-difluoro-4-bora-3a,4a-diaza-s-indacene) chromophores, dyes that have high photoluminescent efficiencies (Φ_{PL} > 0.8), short emission lifetimes (τ < 10 ns) and narrow emission linewidths (full width half maxima, FWHM < 50 nm). However, shifting the emission color of BODIPY into the blue is difficult, and these compounds have intrinsically low triplet energies.[8] These drawbacks make **DIPYR** motifs attractive alternatives for blue fluorescent dopants for use in WOLEDs.

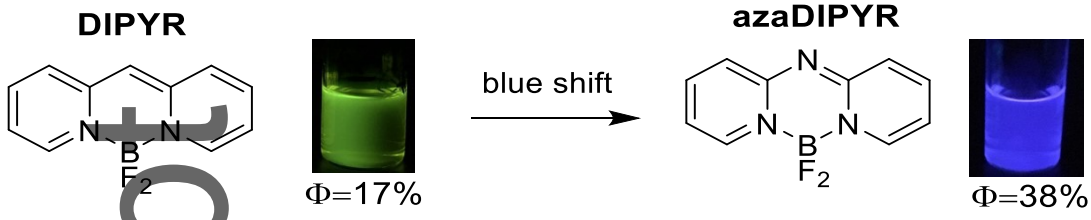

Figure 1. Atomic transmutation of meso-position in DIPYR from methine-bridge to nitrogen-bridge alters the optical properties of the molecule. Photoluminescence quantum yields were obtained in methylcyclohexane.

A simple transmutation from methene carbon to nitrogen converts the green-emissive **DIPYR** to a blue emissive **azaDIPYR** (**aD**) (**Figure 1**). This structural modification stabilizes the energy of the highest occupied molecular orbital (HOMO), but leaves the lowest unoccupied molecular orbital (LUMO) relatively unperturbed, thereby inducing a hypsochromic shift in the emission energy.[9] The emission lifetimes of $\tau < 10$ ns of **DIPYRs** are suitable for use in OLEDs, but the low Φ_{PL} limits the external quantum efficiency (EQE). Previous work on **DIPYR** compounds suggests that benzannulation of the molecular core can improve photoluminescence efficiency, while maintaining the short emission lifetime and narrow linewidths.[9b, 10] We have examined benzannulation along with substitution around the core structure to modify the photophysical properties of a set of **aD** molecules shown in **Figure 2**. Heterocyclic ligands conjugated with boron fluoride, analogous to the **aD** core, have been previously investigated as dyes,[9a, 11] aggregation-induced emitters,[12] and pH sensors,[13] but few studies have been reported on **aD** materials as emitters aside from a citation in the patent literature.[14] Benzannulated derivatives of the **aD** core are potentially useful as blue fluorescent dopants due to their narrow emission profile, nanosecond lifetime, high thermal stability, and high Φ_{PL}. The development of these organic blue-emitting materials is described,

including their synthesis, electrochemical and photophysical characterization, and performance of **2a** in blue OLEDs.

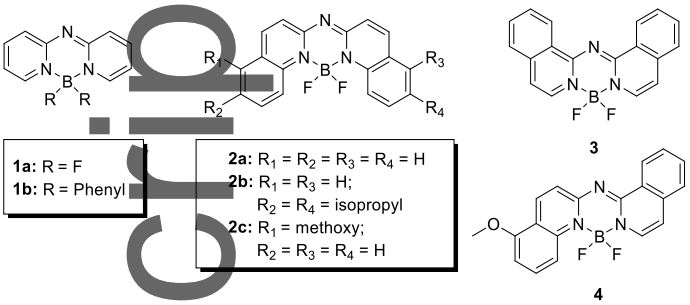

Figure 2. Structures of aza-boron-dipyridylmethene (aD) in this work.

2. Results and Discussion

2.1. Synthesis

The synthesis of the **aD** dyes follows a procedure similar to one previously reported (**Figure 3**).[9a, 13a] A palladium catalyzed coupling reaction of 2-amino and 2-bromo substituted heteroaryl compounds was used to form the desired ligand. The ligand was deprotonated with Hunig's base and treated with $BF_3{\cdot}OEt_2$ to give the **aD** dye. Aryl substituted derivative was prepared by treating the ligand with 2-aminoethoxydiphenyl borate. The products were obtained as microcrystalline solids, which are white-to-yellow for **1a-1b** and bright yellow for **2a-c**, **3** and **4**.

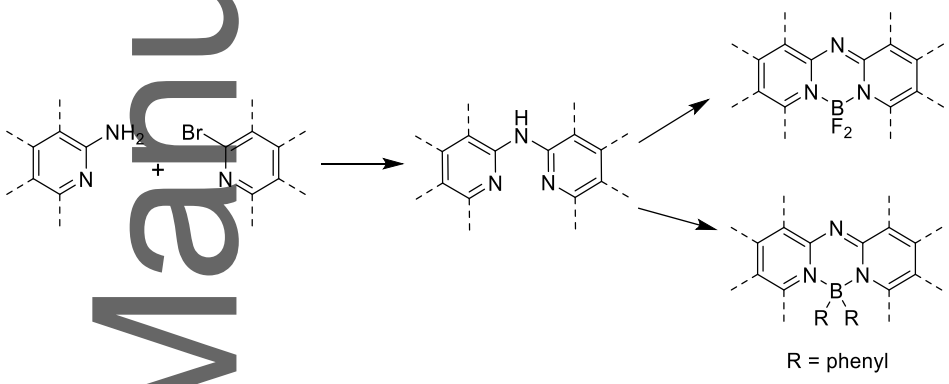

Figure 3. General synthetic scheme to make substituted aza-boron-dipyridylmethene derivatives. Precursors can be pyridyl, quinolyl or isoquinolyl. Detailed procedures are given in the SI.

2.2. Electrochemistry

The electrochemical properties of the **aD** compounds were analyzed by cyclic voltammetry (CV), see **Table 1**. Oxidation is irreversible for all the compounds, whereas reduction is irreversible for **1a-1b** and reversible or quasi-reversible in the benzannulated derivatives, *i.e.* **2a-2c**, **3**, **4**. The oxidation

potentials of the **aD** dyes span a range of 0.72-1.15 V (ΔE_{redox} ~ 400 meV). The reduction potentials span a larger range of -1.91 to -2.59 V (ΔE_{redox} ~ 700 meV). The potentials of the benzannulated derivatives **2a-2c**, **3**, **4** are anodically shifted relative to **1a-1b**, suggesting stabilization of both the filled and vacant frontier molecular orbitals, similar to what is observed in the DIPYR system.[9b] Addition of substituents such as isopropyl (**2b**) or methoxy (**2c** and **4**) groups leads to the cathodic shifts in both oxidation and reduction potentials. For example, the electrochemical potentials of **2c** are shifted relative to **2a** by 0.21 V for oxidation and 0.12 V for reduction.

Table 1. Electrochemical potentials of **1a-1c**, **2a-2c**, **3** and **4.**[a]

	E_{ox} (V)[a]	E_{red} (V)[a]	ΔE_{redox} (V)
1a	+0.92	-2.30	3.22
1b	+0.72	-2.59	3.31
2a	+1.15	-1.91	3.06
2b	+1.08	-1.98	3.06
2c	+1.09	-2.07	3.16
3	+1.10	-2.09	3.19
4	+1.04	-2.14	3.18

[a] Redox potentials obtained from cyclicvoltammetry in acetonitrile with ferrocenium/ferrocene as an internal standard.

2.3. Photophysical characterization

The UV-visible absorption spectra of **1a-1b, 2a-2c, 3** and **4** are shown in **Figure 4**. All of the **aD** compounds have high molar absorptivities (ε ~ 10^4-10^5 M^{-1} cm^{-1}), similar to dyes such as fluorescein, BODIPY (4,4-difluoro-4-bora-3a,4a-diaza-s-indacene), and porphyrin. The **aD** compounds display vibronically structured π-π^* absorption bands between 300-445 nm. The lowest energy absorption

bands in compounds **1a-1b** (λ_{max} = 395-410 nm) are broader than the same transitions in **2a-2c**, **3** and **4** (λ_{max} = 420-445 nm). The decrease in absorption energy in the benzannulated derivatives follows a related decrease in the redox gap, **Table 1**. The full width half maximum (fwhm) for the 0-0 transition in **2a-2c** is narrow (fwhm = 310 cm^{-1}) and **3**, **4** (fwhm = 515 cm^{-1}). Narrow linewidths are similarly observed for the structurally related DIPYR dyes.[9b] The intensity ratios for the 0-0 to 0-1 transitions in **1a-1b** are also smaller than in the benzannulated derivatives. The narrow linewidths along with the large ratio in 0-0 to 0-1 transition intensity suggest that the benzannulated compounds undergo minimal structural change in their excited states.

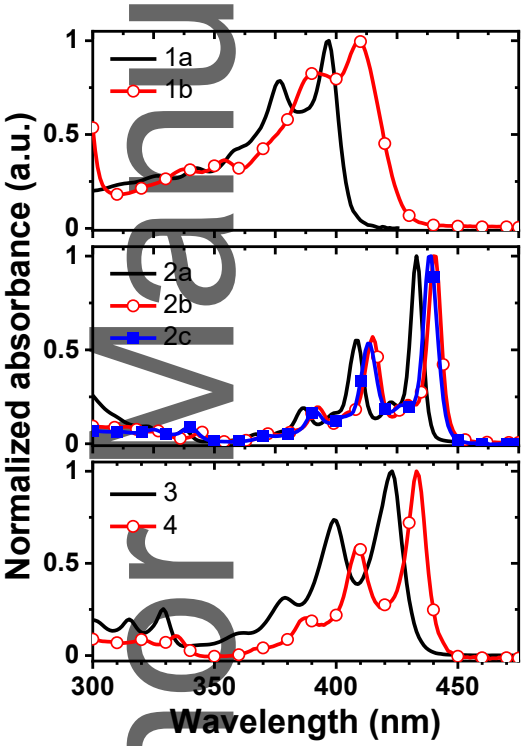

Figure 4. Normalized absorption spectra for **aD** dyes in 2-MeTHF at 298 K. The full width half maximum (fwhm) for the 0-0 transition is narrow in **2a**-**2c**.

Photoluminescence spectra of **1a-1b, 2a**-**2c, 3** and **4** are shown in **Figure 5** and their photophysical data summarized in **Table 2**. The photophysical properties of PMMA films doped at 1 % with the **aD** dyes are similar to those in solution (see SI). The **aD** series give fluorescent emission between λ_{em} = 400-450 nm. Compounds **1a-1b** exhibit violet-to-blue fluorescence spectra that are mirror images of their absorption bands. The Stokes shift increases from 6 nm for **1a** to 20 nm upon addition of phenyl groups in **1b**. The emission profiles of the benzannulated derivatives are bathochromically shifted compared to the non-benzannulated analogs, yet they retain similar vibrational features with an average Stokes shift of ~ 4 nm. Phosphorescence spectra for **aD** compounds taken in 2-MeTHF at 77 K have emission maxima ~ 460 nm for **1a-1b** and 484-502 nm for **2a-2c**, **3** and **4** (**Figure 5**). The $E_{0\text{-}0}$ energies for the lowest excited singlet (S_1) and triplet (T_1) states determined from the peak maxima of the fluorescence and phosphorescence emission spectra, respectively are given in **Table 2**. The material has a cyanine-like property where there is relatively little orbital overlap between the HOMO and LUMO as these orbitals are distributed on different atoms in the molecule (*vide infra*). Thus, Franck-Condon factors are correspondingly small, minimizing vibronic coupling and structural relaxation in the excited state leading to a narrow emission line shape.[15] In addition, this orbital configuration gives rise to the small singlet-triplet gap of these materials.

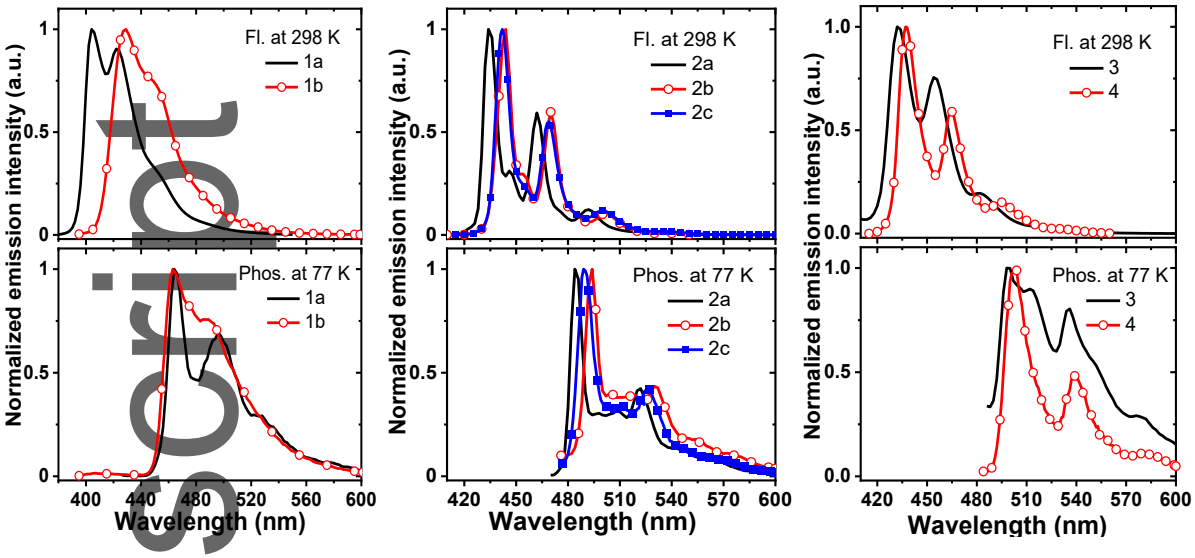

Figure 5. Normalized emission spectra at room temperature (upper plots), and gated phosphorescence emission (bottom plots) recorded after 500 μs delay time at 77 K. Measurements were performed in 2-methyltetrahydrofuran (2-MeTHF).

The photoluminescence quantum yields of the benzannulated compounds in solution and in doped PMMA film are high (Φ_{PL} > 0.80). Polymer films doped at high concentrations (> 1 wt %) display bathochromic shifts, broadened emission spectra and lower quantum yields due to self-absorption, as expected for fluorophores with small Stokes shifts.[16] The excited state lifetimes (τ = 2 to 4 ns) and radiative rates [k_r = (0.93 - 3.2) x 10^8 s^{-1}] are similar across the series, which aligns with common organic fluorophores.[17] However, the non-radiative rates are an order of magnitude higher for the non-benzannulated compounds (k_{nr} = 10^8 s^{-1}) relative to the benzannulated derivatives (k_{nr} = 10^7 s^{-1}). The higher non-radiative rates in the non-benzannulated derivatives are attributed to the faster rates for intersystem crossing (ISC) in these systems.[9b]

Table 2. Summary of the photophysical parameters for **1a-1b**, **2a-2d**, **3** and **4**.[a]

	λ_{abs} (nm)	$\lambda_{em\ max}$ (nm)[b]	Φ_{PL}	τ (ns)	k_r (10^8 s^{-1})[c]	k_{nr} (10^8 s^{-1})[d]	$\lambda_{em\ max}$ (nm)[e]	ΔE_{ST} (eV)
1a	398	404	0.42	2.1	2.0	2.7	464	0.44
1b	409	429	0.30	2.1	1.4	3.4	463	0.34
2a	433	434	0.86	3.3	2.7	0.43	484	0.30
2b	440	444	0.87	3.8	2.3	0.34	494	0.30
2c	441	442	0.84	3.3	2.6	0.49	488	0.27
3	422	432	0.87	3.2	2.8	0.41	498	0.44
4	433	437	0.90	2.8	3.2	0.36	502	0.39

[a] Recorded in 2-MeTHF. [b] Fluorescence measured at 298 K. [c] $k_r = \Phi_{PL}/\tau$. [d] $k_{nr} = (1-\Phi_{PL})/\tau$.

[e] Phosphorescence measured at 77 K.

The singlet and triplet excited state energies were calculated using TD-DFT (B3LYP functional, 6-311G** basis set; see SI for details). Previous studies with BF_2-pyridylmethene and BODIPY dyes have shown that these DFT tends to overestimate the singlet energy but give acceptable values for the triplets.[8l, 9b, 18] Thus, a correction factor of -0.44 eV is needed for the calculated singlet energies to align with the experimental values. The corrected S_1 and uncorrected T_1 state energies predicted by these modeling studies fall within 0.2 eV of spectroscopically determined values. Intersystem

crossing transitions between the S_1 and T_1 states are symmetry forbidden, hence a comparatively slow rate for ISC is expected for $S_1 \rightarrow T_1$. However, the $S_1 \rightarrow T_2$ transition is symmetry allowed, so it is important for the T_2 state to be higher in energy than the S_1 state to prevent ISC *via* $S_1 \rightarrow T_2$ from being competitive with fluorescence. The T_2 state is lower in energy than S_1 in **1a-1b**, but is calculated to be higher than S_1 in **2a-2c**, **3** and **4**. Thus, low quantum yields ($\Phi_{PL} \leq 42\%$) for derivatives **1a-1b** are attributed to exergonic ISC between the S_1 and T_2 states.[9b] Benzannulation in **aD** dyes stabilizes the S_1 state more than the T_2 state, thereby making the $S_1 \rightarrow T_2$ transition thermodynamically unfavorable.

The experimental S_1-T_1 gaps fall in a small range within the **aD** series (ΔE_{ST} = 0.20-0.45 eV). The largest gap is observed for **1a (**ΔE_{ST} = 0.44 eV), where the singlet and triplet gap is similar to that of **DIPYR (**ΔE_{ST} = 0.42 eV) and the benzannulated **DIPYR** derivatives (ΔE_{ST} = 0.43-0.48 eV).[9b] Interestingly, the **aD** benzannulated derivatives have singlet-triplet gaps smaller than the parent **aD** compound (**1a**). Quinoline-based systems (**2a-2d**) maintain a ΔE_{ST} ~ 0.30 eV, whereas isoquinoline systems (**3** and **4**) have a larger gap (ΔE_{ST} ~ 0.40). To determine the origin of the small S_1-T_1 gaps in the **aD** compounds, the extent of spatial overlap (Λ) between the hole and electron natural transition orbitals (NTOs) was calculated for transitions associated with the first excited states (S_1/T_1) (see SI for details). The value of Λ is near unity for strongly localized excitations such as in π-π^* transitions (where the hole and electron involve the same orbitals), giving rise to a large ΔE_{ST}, and Λ = 0 for purely CT transitions with little or no spatial overlap, and thus a small ΔE_{ST}. The computed Λ values and experimental S_1-T_1 gaps of the **aD** series are intermediate between those of a localized transition (anthracene)[19] and a nearly pure CT state (4CzIPN)[20]. Both S_1 and T_1 states in the **aD** compounds show similar degrees of spatial overlap (**1a-1b**, Λ = 0.64-0.68; **2a-2c**, **3** and **4**, Λ = 0.61-

0.68). Λ is 0.84 for anthracene (ΔE_{ST} = 1.46 eV) and 0.29 for 4CzIPN (ΔE_{ST} = 0.10 eV). It is evident that the small Λ range, with ~ 0.15 eV difference between the highest and lowest value, is responsible for the relatively invariant ΔE_{ST} ~ 0.30 eV found in the benzannulated derivatives.

2.4. Electroluminescence

OLEDs were fabricated using compound **2a** as an emissive dopant since its frontier orbital energies and photophysical properties are representative of the **aD** series. The photoluminescence properties of **2a** are also not significantly affected by solvent polarity (see SI), suggesting that a wide range of host materials with different dielectric constants can be employed to equal effect. Compounds reported to be effective hosts for fluorescent blue dopants in OLEDs, N,N′-di(1-naphthyl)-N,N′-diphenyl-(1,1′-biphenyl)-4,4′-diamine (NPD),[21] bis[2-(diphenylphosphino)phenyl] ether oxide (DPEPO)[22], 2,6-bis(3-(carbazol-9-yl)phenyl)pyridine (26DCzPPy)[23] and 4,4′-bis(N-carbazolyl)-1,1′-biphenyl (CBP)[24] were investigated as host materials for **2a**. NPD and DPEPO proved to be poor host materials; NPD films doped at 1 and 10 wt% percent **2a** exhibit a broad photoluminescence between 470 nm to 750 nm, whereas OLEDs with an emissive layer of **2a** doped in DPEPO displayed featureless electroluminescence between 550 nm to 750 nm, which is attributed to emission from an exciplex (see SI). Fortunately, photoluminescence spectra of **2a** doped at 1 and 5 wt % in CBP and 26DCzPPy hosts retain the sharp vibronic emission bands observed in solution. However, the small Stokes shift of **2a** leads to the reabsorption of emitted photons resulting in self-quenching of the fluorophore when doped at higher concentrations. The intensity of the (0-0) photoluminescent emission peak of **2a** (λ_{max} = 453 nm), decreases markedly in 5 wt % films (**Figure**

6). The PL efficiency of CBP and 26DCzPPy films doped at 1 wt % were higher (Φ_{PL} = 0.71 and 0.66, respectively) than those doped at 5 wt % (Φ_{PL}= 0.39 and 0.43, respectively). OLEDs with a 15 nm thick emissive layer (EML) were fabricated with **2a** doped at 1 wt % into CBP or 26DCzPPy. The hole transport layer (HTL) consisted of 10 nm of dipyrazino[2,3,-f:20,30-h]quinoxaline 2,3,6,7,10,11-hexacarbonitrile (HATCN) and 45 nm of 4,4'-cyclohexylidenebis[N,N-bis(4-methylphenyl)benzenamine] (TAPC), whereas the electron transport layer (ETL) comprised of 45 nm of 4,7-diphenyl-1,10-phenanthroline (Bphen) and 1.5 nm of (8-quinolinolato)lithium (LiQ) (1.5 nm). ITO was used as the anode and aluminum as the cathode. The properties of the OLEDs are tabulated in **Table 3**.

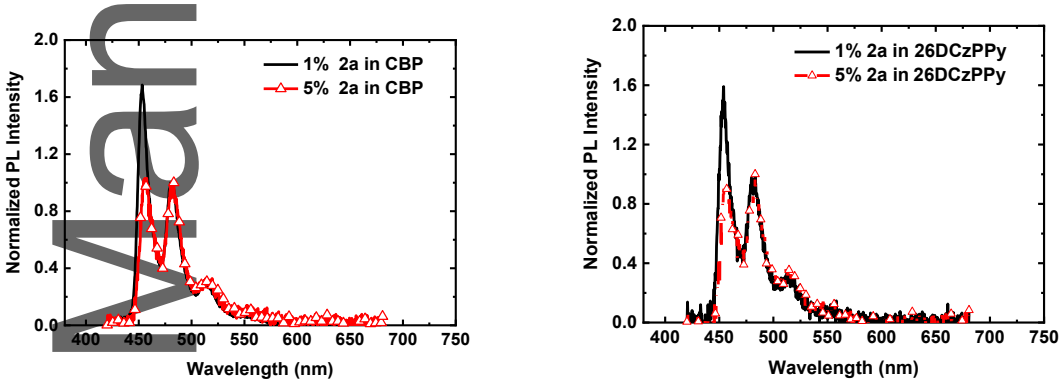

Figure 6: PL emission of 1% and 5% **2a** dopant in CBP and 26DCzPPY host materials.

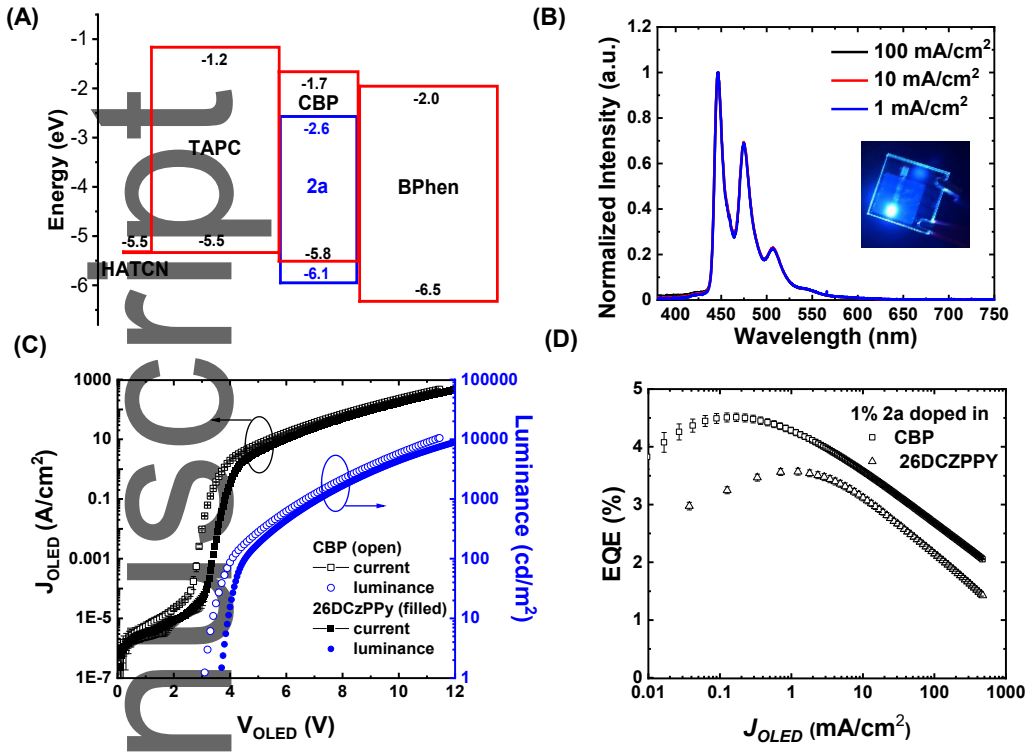

Figure 7. (**A**) Device architecture and energy levels of an OLED with CBP host and **2a** dopant. (**B**) Electroluminescence spectra with increasing current (1-100 mA/cm^2) (**C**) Current vs voltage plots and (**D**) EQE vs current plots for devices using CBP and 26DCzPPy hosts.

Figure 7 shows the device architecture (**Figure 7A**) employing CBP.[25] The electroluminescent emission spectrum in **Figure 7B** retains the sharp and narrow vibronic structure with increasing current density (J = 1-100 mA/cm^2); similar EL spectra are observed in devices using 26DCzPPy (see SI). The turn-on voltage of CBP (V_{on} = 3.5 V; **Figure 7C** and **Table 3**) is lower than 26DCzPPy (V_{on} = 4.5 V). Additionally, the maximum EQE for CBP (4.5 ± 0.2%) is higher than 26DCzPPy (3.5 ± 0.2%), and closer to the theoretical maximum of ~ 5% in a fluorescent OLED on a glass substrate (**Figure 7D**). One drawback in these devices is the steep roll-off in EQE at high current densities, likely caused by hole leakage since the HOMO energy in **2a** (-6.11 eV) is lower than that of either host (CBP, -5.80 eV; 26DCzPPy, 6.05 eV). The small peak observed between wavelengths of 380 and 410 nm with increasing current is attributed to emission from Bphen owing to the hole leakage in these devices (see SI). The observed EQE of 2a in CBP could be due to one of two scenarios: one where the device architecture is optimized and the dopants are isotopically aligned or one where the dopants have significant horizontal alignment but the device architecture has not been completely optimized. Based on the hole leakage observed in these devices, the latter seems more likely. Further studies are needed to determine the molecular orientation of these blue dopants.

Table 3: Properties of OLEDs doped with 1 wt % 2a into CBP and 26DCzPPy hosts.

host	λ_{max} EL (nm)	V_{on} (V)	EQE_{max} (%)	EQE (%, 100 cd/m^2)	EQE (%, 1000 cd/m^2)	CIE coordinate
CBP	445	3.0	4.5[a]	4.1	2.7	(0.15, 0.14)
26DCzPPy	445	3.7	3.5	3.5	2.7	(0.15, 0.14)

[a] Maximum EQE is the average of 7 devices with a standard deviation of 0.13.

3. Conclusion

Substituted aza-boron-dipyridylmethenes (**aD**) were explored as candidates for fluorescent blue dopants in OLEDs. The synthetic flexibility of these materials makes them easy to modify with different substituents to alter their energetics, while also maintaining the high quantum efficiency, small S_1-T_1 gap and small Stokes shift. Seven substituted **aD** compounds were synthesized to study their photophysical and electrochemical properties. All of the compounds display blue fluorescence (λ_{em} = 400 - 500 nm) with quantum efficiencies > 85%. Minimal overlap between the HOMO and LUMO leads to the small singlet-triplet energy gaps of these materials ($\Delta E_{ST} \leq 0.4$ eV). OLEDs prepared using one of these derivatives (**2a**) have low turn-on voltages (3 V) and high efficiency (EQE_{max} = 4.5 ± 0.2%), approaching the maximum theoretical limit of fluorescent OLEDs on glass substrates (EQE = 5%). These studies suggest that **2a** and the other compounds in the **aD** series can serve as fluorescent blue dopants in both monochromatic and white OLEDs. Furthermore, their small single-triplet energy gaps present an opportunity to harvest the triplet excitons to increase the internal quantum efficiency in hybrid fluorescent/phosphorescent white light emitting diodes.

4. Experimental Section

Synthesis: Precursors for **1a-1b** were purchased from Sigma-Aldrich. Aza-boron-dipyridylmethene (aD) synthesis for **1a-1b, 2a-2c, 3** and **4** were prepared using similar coupling reaction synthesis with pyridine, quinoline or isoquinoline core.[13b] The detailed synthesis and characterization of each of the compounds are given in the Supporting Information.

Electrochemical Measurements: Cyclic voltammetry and differential pulsed voltammetry were performed using a VersaSTAT potentiostat measured at 100 mV/s scan. Anhydrous acetonitrile (DriSolv) from Sigma Aldrich was used as the solvent under nitrogen environment, and 0.1 M tetra(n-butyl)ammoniumhexafluorophosphate (TBAF) was used as the supporting electrolyte. A glassy carbon rod was used as the working electrode; a platinum wire was used as the counter electrode, and a silver wire was used as a pseudoreference electrode. The redox potentials are based on values measured from differential pulsed voltammetry and are reported relative to a ferrocenium/ferrocene (Cp_2Fe^+/Cp_2Fe) redox couple used as an internal reference; electrochemical reversibility was determined using cyclic voltammetry.

Photophysical Measurements: All samples in fluid solution were dissolved in 2-methyltetrahydrofuran (2-MeTHF) with absorbance between 0.05-0.15 to prevent reabsorption when performing photoluminescence measurements due to the small Stokes shift in the aD series. Doped poly(methyl methacrylate) thin films were prepared from a solution of poly(methyl methacrylate) (PMMA) in dichloromethane. Samples of **1a**, **2a** and **3** (1 vol %) were dissolved in the PMMA solution and spin coated on a quartz substrate (2 cm x 2 cm) rotating at 700 rpm for 45 seconds. The UV-visible spectra were recorded on a Hewlett-Packard 4853 diode array spectrometer. Steady state fluorescence emission measurements were performed using a QuantaMaster Photon Technology International spectrofluorometer. Gated phosphorescence measurements were carried on the fluorimeter using a 500 microsecond delay on samples at 77 K. All reported spectra are corrected for photomultiplier response. Fluorescence lifetime measurements were performed using an IBH Fluorocube instrument equipped with 331 nm LED and 405 nm laser excitation sources using a time-correlated single photon counting method.

Photoluminescence quantum yields were obtained using the C9920 Hamamatsu integrating sphere system.

Molecular Modeling: All calculations reported in this work were performed using the Q-Chem 5.1 program. Ground-state optimization calculations were performed using B3LYP functional along with 6-311G** basis set. Time dependent density functional theory (TDDFT) calculations on the ground-state optimized geometries were performed using B3LYP/6-311G** level. The singlet energies were corrected by subtracting 0.44 eV as a correction factor commonly used for cyanine-like dyes.[9b]

Device Fabrication: OLEDs were fabricated and tested on glass substrates with pre-patterned, 1 mm wide indium tin oxide (ITO) stripes cleaned by sequential sonication in tergitol, deionized water, acetone, and isopropanol, followed by 15 min UV ozone exposure. Organic materials and metals were deposited at rates of 0.5-2 Å/s through shadow masks in a vacuum thermal evaporator with a base pressure of 10^{-7} Torr. A separate shadow mask was used to deposit 1 mm wide stripes of 100 nm thick Al films perpendicular to the ITO stripes to form the cathode, resulting in a 1 mm^2 device area. The device structure is: glass substrate/70 nm ITO/10 nm dipyrazino[2,3,-f:20,30-h]quinoxaline 2,3,6,7,10,11-hexacarbonitrile (HATCN)/45 nm 4,4'-cyclohexylidenebis [N,N-bis(4-methylphenyl)benzenamine] (TAPC)/1 wt % **2a**: 4,4'-bis(N-carbazolyl)-1,1'-biphenyl (CBP) host/45 nm 4,7-diphenyl-1,10-phenanthroline (BPhen)/ 1.5 nm (8-quinolinolato)lithium (LiQ)/ 100 nm Al. A semiconductor parameter analyzer (HP4156A) and a calibrated large area photodiode that collected all light exiting the glass substrate in the viewing direction were used to measure the J-V-luminance characteristics. The device spectra were measured using a fiber-coupled spectrometer.

Supporting Information

Supplementary Information includes: synthesis of precursors and final compounds, cyclic voltammetry curves, photophysical data of the final compounds in 2-methyltetrahydrofuran, polymer matrix and various OLED host materials, computational data, Organic LED device fabrication and characteristics, TGA, ^{1}HNMR, ^{13}CNMR and CHNS data of final compounds.

Supporting Information is available from the Wiley Online Library or from the author.

Acknowledgements

This project was supported by Universal Display Corporation and the Department of Energy (DE-EE0008244). SRF also acknowledges the Air Force Office of Scientific Research (grant 17RT0908) for financial support. S. Samal for TGA measurements and J.A Collantes for help with the TOC graphic.

Received: ((will be filled in by the editorial staff))
Revised: ((will be filled in by the editorial staff))
Published online: ((will be filled in by the editorial staff))

References

1. (a) Yersin, H., Triplet Emitters for OLED Applications. Mechanisms of Exciton Trapping and Control of Emission Properties. In *Transition Metal and Rare Earth Compounds: Excited States, Transitions, Interactions III*, Springer Berlin Heidelberg: Berlin, Heidelberg, 2004; pp 1-26; (b) Pfeiffer, M.; Forrest, S. R.; Leo, K.; Thompson, M. E., Electrophosphorescent p–i–n Organic Light-Emitting Devices for Very-High-Efficiency Flat-Panel Displays. *Advanced Materials* **2002,** *14* (22), 1633-1636.

2. (a) Adachi, C.; Baldo, M. A.; Forrest, S. R.; Lamansky, S.; Thompson, M. E.; Kwong, R. C., High-efficiency red electrophosphorescence devices. *Applied Physics Letters* **2001,** *78* (11), 1622-1624; (b) Baldo, M. A.; O'Brien, D. F.; You, Y.; Shoustikov, A.; Sibley, S.; Thompson, M. E.; Forrest, S. R., Highly efficient phosphorescent emission from organic electroluminescent devices. *Nature* **1998,** *395* (6698), 151-154; (c) Brooks, J.; Babayan, Y.; Lamansky, S.; Djurovich, P. I.; Tsyba, I.; Bau, R.; Thompson, M. E., Synthesis and Characterization of Phosphorescent Cyclometalated Platinum Complexes. *Inorganic Chemistry* **2002,** *41* (12), 3055-3066; (d) Lamansky, S.; Djurovich, P.; Murphy, D.; Abdel-Razzaq, F.; Kwong, R.; Tsyba, I.; Bortz, M.; Mui, B.; Bau, R.; Thompson, M. E., Synthesis and Characterization of Phosphorescent Cyclometalated Iridium Complexes. *Inorganic Chemistry* **2001,** *40* (7), 1704-1711; (e) Lamansky, S.; Kwong, R. C.; Nugent, M.; Djurovich, P. I.; Thompson, M. E., Molecularly doped polymer light emitting diodes utilizing phosphorescent Pt(II) and Ir(III) dopants. *Org. Electron.* **2001,** *2* (1), 53-62.

3. (a) Shih-Wen, W.; Meng-Ting, L.; Chen, C. H., Recent development of blue fluorescent OLED materials and devices. *Journal of Display Technology* **2005,** *1* (1), 90-99; (b) Lee, J.; Jeong, C.; Batagoda, T.; Coburn, C.; Thompson, M. E.; Forrest, S. R., Hot excited state management for long-lived blue phosphorescent organic light-emitting diodes. *Nature Communications* **2017,** *8* (1), 15566; (c) Adachi, C.; Kwong, R. C.; Djurovich, P.; Adamovich, V.; Baldo, M. A.; Thompson, M. E.; Forrest, S. R., Endothermic energy transfer: A mechanism for generating very efficient high-energy phosphorescent emission in organic materials. *Applied Physics Letters* **2001,** *79* (13), 2082-2084; (d) Zhuang, J.; Li, W.; Su, W.; Liu, Y.; Shen, Q.; Liao, L.; Zhou, M., Highly efficient phosphorescent organic light-emitting diodes using a homoleptic iridium(III) complex as a sky-blue dopant. *Organic Electronics* **2013,** *14* (10), 2596-2601; (e) Klubek, K. P.; Dong, S.-C.; Liao, L.-S.; Tang, C. W.; Rothberg, L. J., Investigating blue phosphorescent iridium cyclometalated dopant with phenyl-imidazole ligands. *Organic Electronics* **2014,** *15* (11), 3127-3136; (f) Kang, Y. J.; Lee, J. Y., High triplet energy electron transport type exciton blocking materials for stable blue phosphorescent organic light-emitting diodes. *Organic Electronics* **2016,** *32*, 109-114; (g) Zhang, L.; Zhang, Y.-X.; Hu, Y.; Shi, X.-B.; Jiang, Z.-Q.; Wang, Z.-K.; Liao, L.-S., Highly Efficient Blue Phosphorescent Organic Light-Emitting Diodes Employing a Host Material with Small Bandgap. *ACS Applied Materials & Interfaces* **2016,** *8* (25), 16186-16191; (h) Seo, J.-A.; Jeon, S. K.; Gong, M. S.; Lee, J. Y.; Noh, C. H.; Kim, S. H., Long lifetime blue phosphorescent organic light-emitting diodes with an exciton blocking layer. *Journal of*

Materials Chemistry C **2015,** *3* (18), 4640-4645; (i) Jeon, S. K.; Lee, J. Y., Four times lifetime improvement of blue phosphorescent organic light-emitting diodes by managing recombination zone. *Organic Electronics* **2015,** *27*, 202-206; (j) Giebink, N.; Dandrade, B.; Weaver, M.; Brown, J.; Forrest, S., Direct evidence for degradation of polaron excited states in organic light emitting diodes. *Journal of Applied Physics* **2009,** *105*, 124514-124514.

4. (a) Reineke, S.; Walzer, K.; Leo, K., Triplet-exciton quenching in organic phosphorescent light-emitting diodes with Ir-based emitters. *Physical Review B* **2007,** *75* (12), 125328; (b) Adachi, C.; Baldo, M. A.; Forrest, S. R.; Thompson, M. E.; A., B. M.; F., O. B. D.; Y., Y.; A., S.; S., S.; E., T. M.; R., F. S., High-efficiency organic electrophosphorescent devices with tris(2-phenylpyridine)iridium doped into electron-transporting materials. *Applied Physics Letters* **2000,** *77* (6), 904-906; (c) Wang, Q.; Aziz, H., Degradation of Organic/Organic Interfaces in Organic Light-Emitting Devices due to Polaron–Exciton Interactions. *ACS Applied Materials & Interfaces* **2013,** *5* (17), 8733-8739; (d) Kim, S.; Bae, H. J.; Park, S.; Kim, W.; Kim, J.; Kim, J. S.; Jung, Y.; Sul, S.; Ihn, S.-G.; Noh, C.; Kim, S.; You, Y., Degradation of blue-phosphorescent organic light-emitting devices involves exciton-induced generation of polaron pair within emitting layers. *Nature Communications* **2018,** *9* (1), 1211; (e) Giebink, N.; D'Andrade, B.; Weaver, M.; Mackenzie, P.; Brown, J.; Thompson, M.; Forrest, S., Intrinsic luminance loss in phosphorescent small-molecule organic light emitting devices due to bimolecular annihilation reactions. *Journal of Applied Physics* **2008,** *103*, 044509-044509; (f) Patel, N. K.; Cina, S.; Burroughes, J. H., High-efficiency organic light-emitting diodes. *IEEE Journal of Selected Topics in Quantum Electronics* **2002,** *8* (2), 346-361.

5. Sun, Y.; Giebink, N. C.; Kanno, H.; Ma, B.; Thompson, M. E.; Forrest, S. R., Management of singlet and triplet excitons for efficient white organic light-emitting devices. *Nature* **2006,** *440* (7086), 908-912.

6. (a) Sun, J. X.; Zhu, X. L.; Peng, H. J.; Wong, M.; Kwok, H. S., Bright and efficient white stacked organic light-emitting diodes. *Org Electron* **2007,** *8*; (b) Sun, N.; Wang, Q.; Zhao, Y.; Chen, Y.; Yang, D.; Zhao, F.; Chen, J.; Ma, D., High-Performance Hybrid White Organic Light-Emitting Devices without Interlayer between Fluorescent and Phosphorescent Emissive Regions. *Advanced Materials* **2014,** *26* (10), 1617-1621; (c) Cho, Y. J.; Yook, K. S.; Lee, J. Y., Cool and warm hybrid white organic light-emitting diode with blue delayed fluorescent emitter both as blue emitter and triplet host. *Sci Reports* **2015,** *5*; (d) Farinola, G. M.; Ragni, R., Electroluminescent materials for white organic light emitting diodes. *Chem Soc Rev* **2011,** *40*; (e) Farinola, G. M.; Ragni, R., Organic emitters for solid state lighting. *Journal of Solid State Lighting* **2015,** *2* (1), 9; (f) Kamtekar, K. T.; Monkman, A. P.; Bryce, M. R., Recent advances in white organic light-emitting materials and devices (WOLEDs). *Adv Mater* **2010,** *22*; (g) Mazzeo, M.; Vitale, V.; Della Sala, F.; Anni, M.; Barbarella, G.; Favaretto, L.; Sotgiu, G.; Cingolani, R.; Gigli, G., Bright white organic light-emitting devices from a single active molecular material. *Adv Mater* **2005,** *17*; (h) Nishide, J.; Nakanotani, H.; Hiraga, Y.; Adachi, C., High-

efficiency white organic light-emitting diodes using thermally activated delayed fluorescence. *Appl Phys Lett* **2014,** *104*; (i) Reineke, S.; Lindner, F.; Schwartz, G.; Seidler, N.; Walzer, K.; Lussem, B.; Leo, K., White organic light-emitting diodes with fluorescent tube efficiency. *Nature* **2009,** *459*; (j) Reineke, S.; Thomschke, M.; Lüssem, B.; Leo, K., White organic light-emitting diodes: Status and perspective. *Rev. Mod. Phys.* **2013,** *85* (3), 1245-1293.

7. Peumans, P.; Yakimov, A.; Forrest, S. R., Small molecular weight organic thin-film photodetectors and solar cells. *J. Appl. Phys.* **2003,** *93* (7), 3693-3723.

8. (a) Loudet, A.; Burgess, K., Bodipy Dyes and Their Derivatives: Syntheses and Spectroscopic Properties. *Chem. Rev.* **2007,** *107* (11), 4891; (b) Chen, J. J.; Conron, S. M.; Erwin, P.; Dimitriou, M.; McAlahney, K.; Thompson, M. E., High-Efficiency BODIPY-Based Organic Photovoltaics. *ACS Applied Materials & Interfaces* **2015,** *7* (1), 662-669; (c) Benstead, M.; Mehl, G. H.; Boyle, R. W., 4,4′-Difluoro-4-Bora-3a,4a-Diaza-S-Indacenes (Bodipys) as Components of Novel Light Active Materials. *Tetrahedron* **2011,** *67* (20), 3573; (d) Bura, T.; Leclerc, N.; Fall, S.; Lévêque, P.; Heiser, T.; Retailleau, P.; Rihn, S.; Mirloup, A.; Ziessel, R., High-Performance Solution-Processed Solar Cells and Ambipolar Behavior in Organic Field-Effect Transistors with Thienyl-Bodipy Scaffoldings. *J. Am. Chem. Soc.* **2012,** *134* (42), 17404; (e) Deng, Y.; Cheng, Y.-y.; Liu, H.; Mack, J.; Lu, H.; Zhu, L.-g., Asymmetrical aza-boron-dipyridomethene derivatives with large Stokes shifts: synthesis and spectroscopic properties. *Tetrahedron Letters* **2014,** *55* (28), 3792-3796; (f) Kamkaew, A.; Lim, S. H.; Lee, H. B.; Kiew, L. V.; Chung, L. Y.; Burgess, K., BODIPY Dyes In Photodynamic Therapy. *Chemical Society reviews* **2013,** *42* (1), 10.1039/c2cs35216h; (g) Karolin, J.; Johansson, L. B. A.; Strandberg, L.; Ny, T., Fluorescence and Absorption Spectroscopic Properties of Dipyrrometheneboron Difluoride (BODIPY) Derivatives in Liquids, Lipid Membranes, and Proteins. *Journal of the American Chemical Society* **1994,** *116* (17), 7801-7806; (h) Kim, B.; Ma, B.; Donuru, V. R.; Liu, H.; Frechet, J. M. J., Bodipy-Backboned Polymers as Electron Donor in Bulk Heterojunction Solar Cells. *Chem. Commun.* **2010,** *46* (23), 4148; (i) Kolemen, S.; Bozdemir, O. A.; Cakmak, Y.; Barin, G.; Erten-Ela, S.; Marszalek, M.; Yum, J. H.; Zakeeruddin, S. M.; Nazeeruddin, M. K.; Gratzel, M.; Akkaya, E. U., Optimization of Distyryl-Bodipy Chromophores for Efficient Panchromatic Sensitization in Dye Sensitized Solar Cells. *Chem. Sci.* **2011,** *2* (5), 949; (j) Kowada, T.; Yamaguchi, S.; Fujinaga, H.; Ohe, K., Near-Infrared Bodipy Dyes Modulated with Spirofluorene Moieties. *Tetrahedron* **2011,** *67* (17), 3105; (k) Kurata, S.; Kanagawa, T.; Yamada, K.; Torimura, M.; Yokomaku, T.; Kamagata, Y.; Kurane, R., Fluorescent quenching-based quantitative detection of specific DNA/RNA using a BODIPY(®) FL-labeled probe or primer. *Nucleic Acids Research* **2001,** *29* (6), e34-e34; (l) Momeni, M. R.; Brown, A., Why Do TD-DFT Excitation Energies of BODIPY/Aza-BODIPY Families Largely Deviate from Experiment? Answers from Electron Correlated and Multireference Methods. *Journal of Chemical Theory and Computation* **2015,** *11* (6), 2619-2632; (m) Orte, A.; Debroye, E.; Ruedas-Rama, M. J.; Garcia-Fernandez, E.; Robinson, D.; Crovetto, L.; Talavera, E. M.; Alvarez-Pez, J. M.; Leen, V.; Verbelen, B.; Cunha Dias de Rezende, L.; Dehaen, W.; Hofkens, J.; Van der Auweraer, M.; Boens, N., Effect of the substitution position (2, 3 or 8) on the

spectroscopic and photophysical properties of BODIPY dyes with a phenyl, styryl or phenylethynyl group. *RSC Advances* **2016,** *6* (105), 102899-102913; (n) Schmitt, A.; Hinkeldey, B.; Wild, M.; Jung, G., Synthesis of the Core Compound of the BODIPY Dye Class: 4,4′ -Difluoro-4-bora-(3a,4a)-diaza-s-indacene. *Journal of Fluorescence* **2009,** *19* (4), 755-758; (o) Sutter, A.; Retailleau, P.; Huang, W.-C.; Lin, H.-W.; Ziessel, R., Photovoltaic performance of novel push-pull-push thienyl-Bodipy dyes in solution-processed BHJ-solar cells. *New Journal of Chemistry* **2014,** *38* (4), 1701-1710; (p) Ulrich, G.; Ziessel, R.; Harriman, A., The Chemistry of Fluorescent Bodipy Dyes: Versatility Unsurpassed. *Angewandte Chemie International Edition* **2008,** *47* (7), 1184-1201; (q) Zhang, X.-F.; Zhu, J., BODIPY parent compound: Excited triplet state and singlet oxygen formation exhibit strong molecular oxygen enhancing effect. *Journal of Luminescence* **2019,** *212*, 286-292; (r) Zhao, J.; Xu, K.; Yang, W.; Wang, Z.; Zhong, F., The triplet excited state of Bodipy: formation, modulation and application. *Chemical Society Reviews* **2015,** *44* (24), 8904-8939.

9. (a) Bañuelos, J.; Arbeloa, F. L.; Martinez, V.; Liras, M.; Costela, A.; Moreno, I. G.; Arbeloa, I. L., Difluoro-boron-triaza-anthracene: a laser dye in the blue region. Theoretical simulation of alternative difluoro-boron-diaza-aromatic systems. *Physical Chemistry Chemical Physics* **2011,** *13* (8), 3437-3445; (b) Golden, J. H.; Facendola, J. W.; Sylvinson M. R, D.; Baez, C. Q.; Djurovich, P. I.; Thompson, M. E., Boron Dipyridylmethene (DIPYR) Dyes: Shedding Light on Pyridine-Based Chromophores. *The Journal of Organic Chemistry* **2017,** *82* (14), 7215-7222; (c) Boyer, J. H.; Haag, A. M.; Sathyamoorthi, G.; Soong, M.-L.; Thangaraj, K.; Pavlopoulos, T. G., Pyrromethene–BF2 complexes as laser dyes: 2. *Heteroatom Chemistry* **1993,** *4* (1), 39-49; (d) Sathyamoorthi, G.; Soong, M.-L.; Ross, T. W.; Boyer, J. H., Fluorescent tricyclic β-azavinamidine–BF2 complexes. *Heteroat. Chem* **1993,** *4* (6), 603-608.

10. Kondo, Y.; Yoshiura, K.; Kitera, S.; Nishi, H.; Oda, S.; Gotoh, H.; Sasada, Y.; Yanai, M.; Hatakeyama, T., Narrowband deep-blue organic light-emitting diode featuring an organoboron-based emitter. *Nature Photonics* **2019**.

11. Araneda, J. F.; Piers, W. E.; Heyne, B.; Parvez, M.; McDonald, R., High Stokes Shift Anilido-Pyridine Boron Difluoride Dyes. *Angewandte Chemie International Edition* **2011,** *50* (51), 12214-12217.

12. (a) Quan, L.; Chen, Y.; Lv, X. J.; Fu, W. F., Aggregation-induced photoluminescent changes of naphthyridine-BF2 complexes. *Chemistry (Weinheim an der Bergstrasse, Germany)* **2012,** *18* (46), 14599-604; (b) Yang, Y.; Su, X.; Carroll, C. N.; Aprahamian, I., Aggregation-induced emission in BF2–hydrazone (BODIHY) complexes. *Chemical Science* **2012,** *3* (2), 610-613.

13. (a) Wang, D.; Liu, R.; Chen, C.; Wang, S.; Chang, J.; Wu, C.; Zhu, H.; Waclawik, E. R., Synthesis, photophysical and electrochemical properties of aza-boron-diquinomethene complexes. *Dyes and Pigments* **2013,** *99* (1), 240-249; (b) Zhu, X.; Huang, H.; Liu, R.; Jin, X.; Li, Y.; Wang, D.; Wang, Q.; Zhu,

H., Aza-boron-diquinomethene complexes bearing N-aryl chromophores: synthesis, crystal structures, tunable photophysics, the protonation effect and their application as pH sensors. *Journal of Materials Chemistry C* **2015,** *3* (15), 3774-3782.

14. Kondakova, M. E.; Deaton, J. C.; Pawlik, T. D.; Giesen, D. J.; Kondakov, D. Y.; Young, R. H.; Royster, T. L.; Comfort, D. L.; Shore, J. D.; R., D. A.; J., S. J.; M., H. C.; F., F. D., Highly efficient fluorescent-phosphorescent triplet-harvesting hybrid organic light-emitting diodes. *Journal of Applied Physics* **2010,** *107* (1), 014515.

15. (a) Kondo, Y.; Yoshiura, K.; Kitera, S.; Nishi, H.; Oda, S.; Gotoh, H.; Sasada, Y.; Yanai, M.; Hatakeyama, T., Narrowband deep-blue organic light-emitting diode featuring an organoboron-based emitter. *Nature Photonics* **2019,** *13*; (b) Oda, S.; Kawakami, B.; Kawasumi, R.; Okita, R.; Hatakeyama, T., Multiple Resonance Effect-Induced Sky-Blue Thermally Activated Delayed Fluorescence with a Narrow Emission Band. *Organic Letters* **2019,** *21* (23), 9311-9314.

16. (a) Ding, H.; Yu, H.; Dong, Y.; Tian, R.; Huang, G.; Boothman, D. A.; Sumer, B. D.; Gao, J., Photoactivation Switch from Type II to Type I Reactions by Electron-Rich Micelles for Improved Photodynamic Therapy of Cancer Cells Under Hypoxia. *Journal of controlled release : official journal of the Controlled Release Society* **2011,** *156* (3), 276-280; (b) Stopel, M. H. W.; Blum, C.; Subramaniam, V., Excitation Spectra and Stokes Shift Measurements of Single Organic Dyes at Room Temperature. *The Journal of Physical Chemistry Letters* **2014,** *5* (18), 3259-3264; (c) Sissa, C.; Painelli, A.; Terenziani, F.; Trotta, M.; Ragni, R., About the origin of the large Stokes shift in aminoalkyl substituted heptamethine cyanine dyes. *Physical Chemistry Chemical Physics* **2020,** *22* (1), 129-135.

17. (a) Berezin, M. Y.; Achilefu, S., Fluorescence lifetime measurements and biological imaging. *Chemical reviews* **2010,** *110* (5), 2641-2684; (b) Ostroverkhova, O., Organic Optoelectronic Materials: Mechanisms and Applications. *Chemical Reviews* **2016,** *116* (22), 13279-13412.

18. Charaf-Eddin, A.; Le Guennic, B.; Jacquemin, D., Excited-states of BODIPY–cyanines: ultimate TD-DFT challenges? *RSC Advances* **2014,** *4* (90), 49449-49456.

19. Schols, S.; Kadashchuk, A.; Heremans, P.; Helfer, A.; Scherf, U., Triplet excitation scavenging as method to control the triplet concentration. *Proceedings of SPIE - The International Society for Optical Engineering* **2009,** *7415*.

20. (a) Nakanotani, H.; Masui, K.; Nishide, J.; Shibata, T.; Adachi, C., Promising operational stability of high-efficiency organic light-emitting diodes based on thermally activated delayed fluorescence. *Sci. Rep.* **2013,** *3*, 2127-2127; (b) Cho, Y. R.; Cha, S. J.; Suh, M. C., Ideal combination of the host and dopant materials showing thermally activated delayed fluorescent behavior. *Synth. Met.* **2015,** *209*, 47-54.

21. (a) Zhang, X. H.; Liu, M. W.; Wong, O. Y.; Lee, C. S.; Kwong, H. L.; Lee, S. T.; Wu, S. K., Blue and white organic electroluminescent devices based on 9,10-bis(2′-naphthyl)anthracene. *Chemical Physics Letters* **2003,** *369* (3), 478-482; (b) Slyke, S. A. V.; Chen, C. H.; Tang, C. W., Organic electroluminescent devices with improved stability. *Applied Physics Letters* **1996,** *69* (15), 2160-2162; (c) Guo, F.; Ma, D.; Wang, L.; Jing, X.; Wang, F., High efficiency white organic light-emitting devices by effectively controlling exciton recombination region. *Semiconductor Science and Technology* **2005,** *20* (3), 310-313.

22. Kumar, M.; Pereira, L., Effect of the Host on Deep-Blue Organic Light-Emitting Diodes Based on a TADF Emitter for Roll-Off Suppressing. *Nanomaterials (Basel, Switzerland)* **2019,** *9* (9), 1307.

23. Su, S.-J.; Sasabe, H.; Takeda, T.; Kido, J., Pyridine-Containing Bipolar Host Materials for Highly Efficient Blue Phosphorescent OLEDs. *Chemistry of Materials* **2008,** *20* (5), 1691-1693.

24. (a) Bagnich, S. A.; Athanasopoulos, S.; Rudnick, A.; Schroegel, P.; Bauer, I.; Greenham, N. C.; Strohriegl, P.; Köhler, A., Excimer Formation by Steric Twisting in Carbazole and Triphenylamine-Based Host Materials. *The Journal of Physical Chemistry C* **2015,** *119* (5), 2380-2387; (b) Bagnich, S. A.; Rudnick, A.; Schroegel, P.; Strohriegl, P.; Köhler, A., Triplet energies and excimer formation in meta- and para-linked carbazolebiphenyl matrix materials. *Philos Trans A Math Phys Eng Sci* **2015,** *373* (2044), 20140446.

25. Yoshida, H.; Yoshizaki, K., Electron affinities of organic materials used for organic light-emitting diodes: A low-energy inverse photoemission study. *Organic Electronics* **2015,** *20*, 24-30.

Table of Contents Entry

A. C. Tadle, Dr. K. A. El Roz, C. H. Soh, D. S. M. Ravinson, Dr. P. I. Djurovich, Dr. S. R. Forrest, Dr. M. E. Thompson*

Tuning the Photophysical and Electrochemical Properties of Aza-boron-dipyridylmethene Compounds for Fluorescent Blue OLEDs

ToC figure ((Please choose one size: 55 mm broad × 50 mm high **or** 110 mm broad × 20 mm high. Please do not use any other dimensions))

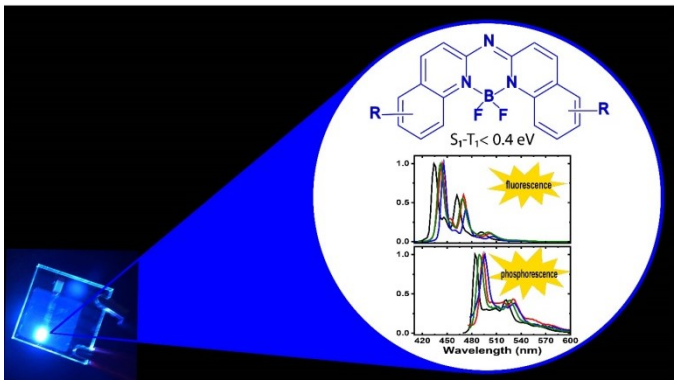

A class of blue fluorescent boron-aza-dipyridylmethene with small excited state energy gaps (ΔE_{ST} < 400 meV) and high photoluminescence efficiencies (Φ_{PL} > 0.8) lead to blue monochromatic devices with external quantum efficiencies close to the theoretical maximum. The synthetic and optical tunability along with the thermal and chemical stability of these materials make them viable options for organic optoelectronics.